INTERNATIONAL JOURNAL OF MECHANICS
DOI: 10.46300/9104.2026.20.2 Volume 20, 2026

Optimizing MRR and Electrode Wear in Ultrasonic EDM: A Multi-Criteria Approach Using NSGA-II and MABAC

Dinh Van Thanh[1], Le Thu Quy[2], Do Thi Tam[3], Vu Ngoc Pi[3], Tran Thi Phuong Thao[3,*]
[1]Electronics and Electrical Department, East Asia University of Technology, Trinh Van Bo Street, Hanoi City 12000, Vietnam
[2]National Research Institute of Mechanical Engineering, 04 Pham Van Dong, Ha Noi City 11309, Vietnam
[3]Faculty of Mechanical Engineering, Thai Nguyen University of Technology, 3/2 Street, Tich Luong Ward, Thai Nguyen City 24000, Vietnam

**Corresponding Author*

Received: May 9, 2025. Revised: July 27, 2025. Accepted: August 28, 2025. Published: April 8, 2026.

Abstract— Ultrasonic-assisted Electrical Discharge Machining (UV-EDM) has emerged as a promising technique for improving machining efficiency and electrode life, particularly when processing hard conductive materials. This study presents a hybrid multi-criteria optimization framework that integrates Non-dominated Sorting Genetic Algorithm II (NSGA-II) and the Multi-Attributive Border Approximation Area Comparison (MABAC) method to optimize two conflicting performance measures: Material Removal Rate (MRR) and Electrode Wear Rate (EWR).

A Box–Behnken Design (BBD) experimental matrix was developed with five input parameters: ultrasonic vibration amplitude, pulse-on time, pulse-off time, peak current, and servo voltage. Experiments were conducted using a Sodick A30 EDM machine with a custom-designed ultrasonic horn and copper electrodes on 90CrSi tool steel. Surrogate models for MRR and EWR were constructed using Gaussian Process Regression (GPR), enabling efficient evaluation of process responses during the optimization phase.

NSGA-II was employed to generate a diverse Pareto front representing trade-offs between MRR and EWR. Subsequently, the MABAC method was applied to rank the Pareto-optimal solutions and identify the most balanced process setting. The best compromise solution offered a high MRR while maintaining a low EWR, demonstrating the effectiveness of the proposed hybrid approach in balancing productivity and electrode sustainability in UV-EDM operations.

Keywords— Ultrasonic EDM; Material Removal Rate (MRR); Electrode Wear Rate (EWR); NSGA-II; MABAC; Multi-objective optimization; Gaussian Process Regression (GPR); EDM process parameters.

I. INTRODUCTION

ELECTRICAL Discharge Machining (EDM) has long been regarded as a vital process for shaping hard, conductive materials with complex geometries. However, conventional EDM faces inherent limitations in terms of low material removal rate (MRR) and excessive electrode wear rate (EWR), especially when dealing with high-strength alloys. In recent years, ultrasonic vibration-assisted EDM (UV-EDM) has gained significant attention for its ability to enhance machining performance by superimposing high-frequency vibration on the tool or workpiece.

Several studies have demonstrated the positive impact of ultrasonic vibration on the EDM process. The study, [1], proposed a novel EDM method using longitudinal-torsional ultrasonic vibration (LTV) applied to micro-holes, resulting in improved machining efficiency and hole accuracy. The study, [2], observed bubble behavior during ultrasonic-assisted EDM and concluded that cavitation contributes to more stable spark discharge and effective debris removal. The study, [3], also confirmed that ultrasonic vibration enhances spark frequency and reduces arcing by promoting better flushing conditions.

Mechanistic understanding has been explored in [4], analyzed material removal mechanisms in ultrasonic EDM in gas media and found that melting, spalling, and bubble collapse jointly affect MRR. The study, [5], introduced laminated electrodes for machining enclosed microgrooves, achieving improved surface finish and reduced tool wear under ultrasonic excitation. Finite element modeling by [6], provided additional insight into temperature and stress distributions during vibration-assisted machining.

Synchronization of vibration with discharge pulses has also been explored. The study, [7], studied the effects of pulse-vibration synchronization and reported increased discharge

uniformity. The study, [8], combined micro-powder suspension with ultrasonic vibration in the dielectric fluid and used a Taguchi approach to optimize micro-EDM responses. The study, [9], systematically analyzed process parameters and found that vibration amplitude and pulse duration were key influencers on both MRR and dimensional accuracy.

Surface generation mechanisms under UV-EDM have also been a focus. The study, [10], examined crater formation and debris dynamics, while, [11], applied ultrasonic vibration to $Si_3 N_4$ ceramics, resulting in improved machining rates and reduced micro-cracks. More recently, [12], emphasized the role of cavitation in modifying surface topography and reducing thermal damage.

Hybrid enhancements such as magnetic assistance, [13], simultaneous tool–workpiece vibration, [14], and multi-mode excitation, [15], have been tested to further augment process efficiency. The study, [16], validated the tool vibration effects both numerically and experimentally. The study, [17], reported enhanced machinability of PCD materials using ultrasonic vibrating electrodes. The study, [18], applied the Taguchi method to optimize ultrasonic micro-EDM and confirmed significant improvements in tool life and consistency.

Moreover, the effects of ultrasonic vibration on electrode wear have been specifically investigated. The study, [19], observed that workpiece vibration leads to more uniform wear patterns. The study, [20], developed thermodynamic models to simulate temperature distribution in vertical UV-EDM. The study, [21], performed multi-objective optimization for micro-EDM of Ti-6Al-4V, balancing material removal with electrode degradation.

Early experimental work by [22], confirmed the effectiveness of tool vibration in reducing electrode wear during EDM of WC-Co. The study, [23], compared ultrasonic vibration and magnetic field assistance, concluding that ultrasonic excitation is more effective for improving both MRR and tool life.

Despite these advancements, most existing studies have focused either on single-objective optimization or unstructured parameter tuning. The complex trade-off between MRR and EWR, particularly under ultrasonic conditions, remains underexplored using systematic multi-criteria decision-making (MCDM) frameworks.

To address this gap, the present study proposes a hybrid approach that combines Non-dominated Sorting Genetic Algorithm II (NSGA-II) for Pareto optimization with the Multi-Attributive Border Approximation Area Comparison (MABAC) method for ranking the non-dominated solutions. The goal is to simultaneously maximize MRR and minimize EWR in UV-EDM of hard tool steels. By integrating evolutionary search and structured decision analysis, the proposed framework aims to support practical process planning where productivity and electrode life must be balanced.

II. Methodology

This study proposes a four-stage hybrid methodology combining experimental design, surrogate modeling, multi-objective evolutionary optimization, and multi-criteria decision-making. The goal is to simultaneously optimize Material Removal Rate (MRR) and Electrode Wear Rate (EWR) in Ultrasonic Vibration-Assisted Electrical Discharge Machining (UV-EDM).

A. Experimental Design and Input Variables

A five-factor Box–Behnken Design (BBD) was employed to construct the experimental matrix. The selected input parameters include ultrasonic vibration amplitude (A), pulse-on time (T_{on}), pulse-off time (T_{off}), peak current (IP), and servo voltage (SV). These factors were studied at three levels (−1, 0, +1) as shown in Table I.

Table I. Input parameters and their levels

Factor	Description	Unit	Level -1	Level 0	Level +1
A	Ultrasonic vibration amplitude	µm	1.15	1.6	1.75
B	Pulse-on time (T_{on})	µs	8	12	16
C	Pulse-off time (T_{off})	µs	8	12	16
D	Peak current (IP)	A	3	5	7
E	Servo voltage (SV)	V	3	5	7

B. Surrogate Modeling with Gaussian Process Regression

To efficiently explore the design space without excessive physical experimentation, Gaussian Process Regression (GPR) was employed as a surrogate modeling technique for both response variables: Material Removal Rate (MRR) and Electrode Wear Rate (EWR). GPR is a non-parametric, probabilistic machine learning method that models the distribution over functions and provides not only point predictions but also uncertainty quantification.

Let x = [A, T_{on}, T_{off}, I_P, SV] denote the vector of input parameters. GPR assumes that the response y(x) follows a Gaussian distribution, and any finite collection of these variables has a joint multivariate Gaussian distribution. The model is fully specified by its mean function m(x) and covariance function (or kernel) k(x,x′), expressed as:

$$y(x) \sim \mathcal{GP}\left(0, k(x, x')\right) \quad (1)$$

In this study, the squared exponential kernel (also known as radial basis function, RBF) was used due to its smoothness properties and capability to handle nonlinear relationships:

$$k(x, x') = \sigma_f^2 exp\left(-\frac{1}{2}(x - x')\Lambda^{-1}(x - x')\right) \quad (2)$$

Where σ_f^2 is the signal variance, and Λ is a diagonal matrix of length scales for each input dimension.

The GPR models were trained using experimental data collected from 46 runs of the Box–Behnken Design. Hyperparameters of the models (length scales, signal noise, etc.) were optimized by maximizing the log marginal likelihood. The models were validated using 10-fold cross-validation, and their predictive accuracy was assessed using:

- Root Mean Square Error (RMSE),
- Mean Absolute Error (MAE),
- Coefficient of Determination (R^2).

The resulting GPR models were used as fitness functions in the subsequent optimization step to rapidly evaluate thousands of parameter combinations with high fidelity.

C. Pareto Optimization Using NSGA-II

To identify the optimal process parameters that balance the two conflicting objectives—maximizing MRR and minimizing EWR—the study employed the Non-dominated Sorting Genetic Algorithm II (NSGA-II). NSGA-II is a widely used evolutionary algorithm designed for solving multi-objective optimization problems by approximating the Pareto front with high diversity and convergence quality.

The optimization problem was defined as:

$$\text{Maximize } f_1(x) = MRR_{GPR}(x) \quad (3)$$

$$\text{Minimize } f_2(x) = EWR_{GPR}(x) \quad (4)$$

Where x = [A, T_{on}, T_{off}, I_P, SV] is the decision variable vector, and MRR_{GPR}, EWR_{GPR} are predicted outputs from the GPR models.

To standardize the objectives within the NSGA-II framework, the first objective was negated (so that both objectives became minimization problems).

Algorithmic Components

NSGA-II employs three key mechanisms:

1. Fast non-dominated sorting: Classifies individuals into multiple Pareto fronts based on dominance relations.
2. Crowding distance computation: Preserves diversity by estimating the density of solutions surrounding a candidate.
3. Elitism: Retains the best individuals across generations to improve convergence stability.

Parameter Settings

The NSGA-II algorithm was implemented in MATLAB and configured with the following parameters: The population size: 100, the number of generations: 150, the crossover probability: 0.9, and the mutation probability: 0.1.

Constraints on the decision variables were imposed according to the experimental design bounds (see Table I).

Output and Interpretation

The algorithm produced a Pareto front of non-dominated solutions, each representing a trade-off between high MRR and low EWR. These solutions were subsequently evaluated using the MABAC decision-making method (Section 2.4) to identify the most balanced and practically viable machining configuration.

D. Decision-Making Using the MABAC Method

To select the most suitable solution from the Pareto-optimal set generated by NSGA-II, the Multi-Attributive Border Approximation Area Comparison (MABAC) method, proposed by [24], was applied. MABAC evaluates alternatives by measuring their distances from a reference zone known as the border approximation area (BAA). The following steps describe the procedure to implement the MABAC method in this study:

Step 1: Construct the initial decision matrix

$$X = \begin{bmatrix} r_{11} & \cdots & r_{1j} & \cdots & r_{1n} \\ \vdots & \ddots & \vdots & \ddots & \vdots \\ r_1 & \cdots & r_{ij} & \cdots & r_{in} \\ \vdots & \ddots & \vdots & \ddots & \vdots \\ r_{m1} & \cdots & r_{mj} & \cdots & r_{mn} \end{bmatrix}_{m\times n} \quad (5)$$

Step 2: Normalize the decision matrix:

- For beneficial criteria (e.g., MRR):

$$r_{ij}^{*} = \frac{r_{ij} - r_i^{-}}{r_i^{+} - r_i^{-}} \quad (6)$$

- For non-beneficial criteria (e.g., EWR):

$$r_{ij}^{*} = \frac{r_{ij} - r_i^{+}}{r_i^{-} - r_i^{+}} \quad (7)$$

Where $r_i^{+} = max(r_1, r_2, \ldots, r_m)$ and $r_i^{-} = min(r_1, r_2, \ldots, r_m)$.

Step 3: Calculate the weighted normalized matrix by

$$v_{ij} = w_j + w_j \times r_{ij}^{*} \quad (8)$$

Step 4: Compute the border approximation area by:

$$g_j = \left(\prod_{i=1}^{m} v_{ij}\right)^{1/m} \quad (9)$$

Step 5: Calculate the distance from the border approximation area by:

$$q_{ij} = v_{ij} - g_i \quad (101)$$

Step 6: Compute the total score for each alternative by:

$$S_i = \sum_{j=1}^{n} q_{ij} \; i = 1, 2, \ldots, m \quad (11)$$

Step 7: Rank the alternatives by maximizing S_i. The alternative with the highest score is considered the most balanced and optimal solution, offering the best compromise between competing objectives.

E. Entropy Method for Criteria Weight Determination

In multi-criteria decision-making problems, the weight assignment for each criterion plays a crucial role in determining the final ranking of alternatives. To avoid subjectivity and ensure an objective assessment of importance, this study employed the Entropy method to determine the weights of the criteria—specifically, Material Removal Rate (MRR) and Electrode Wear Rate (EWR)—before implementing the MABAC method.

The Entropy method is an information-theoretic approach that measures the degree of divergence or variation in the

decision matrix. The lower the entropy of a criterion, the higher its discriminative power, and consequently, the greater its weight in decision-making. The following steps were used to implement the Entropy method, [25]:

Step 1: Normalize the decision matrix

Let x_{ij} denote the value of the j^{th} criterion for the i^{th} alternative. The normalized value p_{ij} is calculated as:

$$p_{ij} = \frac{x_{ij}}{m+\sum_{i=1}^{m} x_{ij}^2} \quad (12)$$

where m is the number of alternatives, n is the number of criteria, and x_{ij} is the raw value in the decision matrix.

This normalization ensures that all criteria are scaled uniformly across alternatives.

Step 2: Compute the entropy value of each criterion

The entropy m_{ej} for each criterion j is calculated using the following formula:

$$me_j = -\sum_{i=1}^{m}[p_{ij} \times ln(p_{ij})] - (1 - \sum_{i=1}^{m} p_{ij}) \times ln(1 - \sum_{i=1}^{m} p_{ij}) \quad (13)$$

This entropy value quantifies the level of uncertainty or uniformity associated with each criterion. A lower entropy indicates higher information diversity and, therefore, greater importance.

Step 3: Determine the objective weights

The weight w_j for each criterion j is calculated by:

$$w_j = \frac{1-me_j}{\sum_{j=1}^{m}(1-me_j)} \quad (14)$$

This formula ensures that the weights are normalized such that their sum equals 1.

In this study, the Entropy-derived weights were used as the objective weighting scheme for evaluating trade-offs between MRR and EWR in the MABAC-based selection. This approach ensures that the final decision is not only grounded in data but also free from bias introduced by subjective judgment.

III. Experimental Work

The experimental investigation was conducted using a Sodick A30 EDM machine, modified to incorporate ultrasonic vibration through a custom-designed ultrasonic horn, which was developed and fabricated specifically for this study as described in [25]. The experimental setup is shown schematically in Figure 1. Ultrasonic vibration was transmitted to the tool electrode at a fixed frequency of 20 kHz, with vibration amplitude controlled by an external signal generator and amplifier. Copper electrodes were used due to their favorable electrical and thermal properties in EDM applications. The workpiece material was 90CrSi tool steel, selected for its high hardness and relevance in tooling applications. Machining was performed in a bath of Total Diel MS 7000 dielectric oil, a low-viscosity insulating fluid commonly used in precision EDM.

The five process parameters selected as input variables were: ultrasonic vibration amplitude (A, µm), pulse-on time (T_{on}, µs), pulse-off time (T_{off}, µs), peak current (I_P, A), and servo voltage (SV, V). The measured output responses were the Material Removal Rate (MRR, g/h) and the Electrode Wear Rate (EWR, g/h). MRR was calculated by measuring the difference in workpiece weight before and after machining, divided by the machining time. Similarly, EWR was determined by measuring the mass loss of the copper electrode. All weight measurements were performed using a precision electronic balance with an accuracy of ±0.1 mg, and each experiment was repeated three times to ensure repeatability. The average of three trials was recorded for each run.

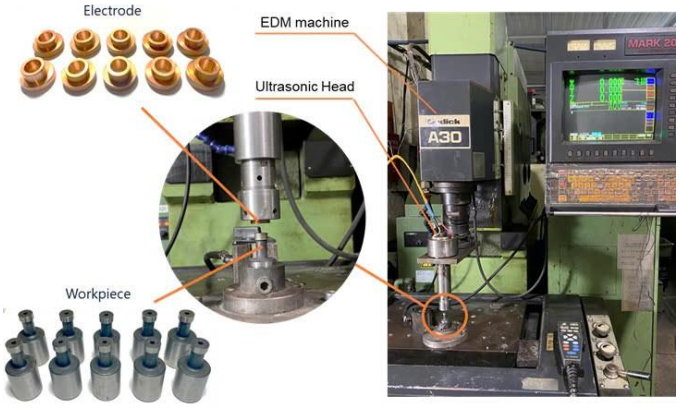

Fig 1: Experimental setup

The experimental plan was constructed based on the Box–Behnken Design (BBD), covering the five selected input variables at three levels (−1, 0, +1), resulting in a total of 46 experimental runs. Each run corresponds to a unique combination of parameter settings, enabling the modeling of both main effects and interactions without requiring a full factorial design. The complete input matrix and corresponding experimental results for MRR and EWR are presented in Table II – Experimental matrix and results, which were used to develop the Gaussian Process Regression (GPR) models for subsequent multi-objective optimization.

Table II: Input parameters and output results

Trial	A	T_{on}	T_{off}	IP	SV	MRR (g/h)	EWR (g/h)
1	1.15	12	12	5	5	3.374	0.013
2	1.15	16	12	7	5	5.004	0.038
3	1.15	8	12	3	5	1.086	0.011
4	1.15	12	12	3	7	1.994	0.010
5	1.6	12	12	3	5	0.836	0.019
6	1.15	16	12	3	5	1.191	0.003
7	1.15	8	8	5	5	1.493	0.028
8	1.15	16	8	5	5	3.354	0.007
9	1.15	8	12	5	7	1.417	0.026

10	1.15	8	16	5	5	1.360	0.029
11	1.15	12	12	5	5	3.292	0.015
12	1.15	12	8	5	3	3.546	0.032
13	1.15	12	12	7	3	3.729	0.042
14	1.15	16	16	5	5	3.098	0.005
15	1.15	12	12	5	5	3.275	0.026
16	1.75	12	12	7	5	2.542	0.028
17	1.15	12	12	5	5	3.249	0.017
18	1.15	12	8	5	7	3.349	0.024
19	1.6	16	12	5	5	1.972	0.011
20	1.6	12	8	5	5	2.506	0.023
21	1.75	12	12	5	7	1.669	0.020
22	1.15	8	12	7	5	1.392	0.035
23	1.75	8	12	5	5	0.305	0.035
24	1.6	12	16	5	5	2.373	0.018
25	1.15	12	8	7	5	4.054	0.046
26	1.15	12	16	5	3	3.252	0.027
27	1.15	12	12	5	5	3.313	0.029
28	1.15	12	8	3	5	1.996	0.018
29	1.15	16	12	5	3	2.947	0.032
30	1.15	16	12	5	7	3.517	0.023
31	1.15	12	16	7	5	3.736	0.035
32	1.15	12	16	5	7	3.202	0.018
33	1.75	12	16	5	5	2.156	0.032
34	1.15	12	12	7	7	3.609	0.020
35	1.75	12	8	5	5	2.322	0.021
36	1.6	12	12	7	5	2.720	0.032
37	1.15	8	12	5	3	1.349	0.029
38	1.15	12	12	5	5	3.390	0.027
39	1.6	12	12	5	7	2.210	0.006
40	1.75	16	12	5	5	1.828	0.014
41	1.6	8	12	5	5	0.361	0.025
42	1.6	12	12	5	3	2.372	0.032
43	1.15	12	12	3	3	1.275	0.007
44	1.75	12	12	3	5	0.916	0.020
45	1.15	12	16	3	5	1.914	0.016
46	1.75	12	12	5	3	2.034	0.025

IV. Results and Discussion

A. Pareto-Optimal Solutions via NSGA-II and GPR Surrogates

The combination of Gaussian Process Regression (GPR) models and the NSGA-II algorithm resulted in a well-distributed set of Pareto-optimal solutions that reflect the inherent trade-off between Material Removal Rate (MRR) and Electrode Wear Rate (EWR). As illustrated in Figure 2, the Pareto front exhibits a typical convex shape where any improvement in MRR is accompanied by an increase in EWR, and vice versa.

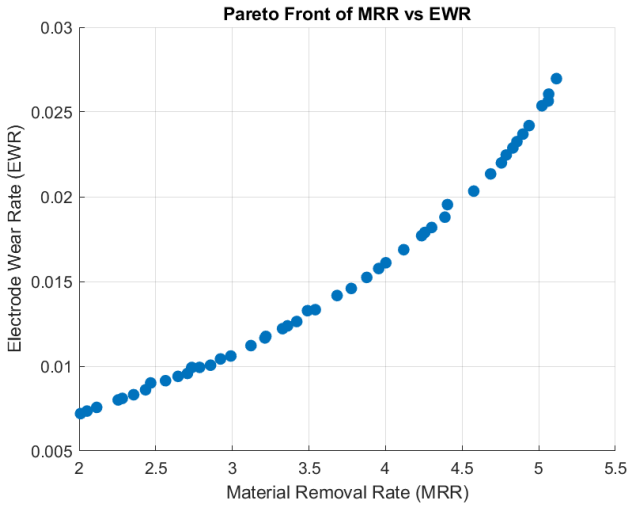

Fig 2: Pareto front of MRR vs EWR

The predicted MRR values across the Pareto front ranged approximately from 2.0 to 5.1 g/h, while the corresponding EWR values ranged from 0.007 to 0.027 g/h. This behavior indicates that higher productivity (increased MRR) tends to accelerate electrode degradation. This trade-off is especially important in industrial settings where both machining efficiency and tool life are critical.

The richness and smoothness of the Pareto front confirm the capability of the GPR models to accurately predict responses over the design space, and the effectiveness of NSGA-II in capturing a wide set of feasible solutions.

B. Multi-Criteria Evaluation Using MABAC Method

To select the most balanced solution from the Pareto front, the MABAC method was employed using objective weights derived from the Entropy method: 0.3388 for MRR and 0.6612 for EWR. These weights reflect the relative importance of electrode life over material removal in this study.

The MABAC procedure involved computing the weighted normalized matrix v_{ij}, the geometric mean for each criterion g_j, and the distance of each alternative q_{ij} from the border approximation area. The total score S_i for each alternative was obtained by aggregating the criterion-wise distances.

From the MABAC analysis (Table III), Trial 8 emerged as the most preferred alternative with the highest score, S_i=0.2714, achieving a Material Removal Rate of 3.354 g/h

and an Electrode Wear Rate of 0.007 g/h. Other well-performing solutions included Trial 2 (Rank 2, S_i=0.2617) and Trial 1 (Rank 4, S_i=0.2242).

Notably, alternatives with extreme values—very high MRR or very low EWR—often exhibited large negative deviations in one criterion, thus receiving lower overall MABAC scores. For example, Trial 22, despite having a favorable EWR, scored poorly due to low MRR and ranked 44th out of 46.

Table III: Calculated results and ranking by MABAC

Trial.	w_{ij}		v_{ij}		g_{ij}		q_{ij}		S_i	Rank
	MRR	EWR	MRR	EWR	MRR	EWR	MRR	EWR		
1	0.3388	0.6612	0.5985	1.0931	0.5185	0.9489	0.0800	0.1442	0.2242	4
2	0.3388	0.6612	0.4066	1.3225	0.5185	0.9489	-0.1119	0.3735	0.2617	2
3	0.3388	0.6612	0.6185	0.7711	0.5185	0.9489	0.1000	-0.1778	-0.0778	36
4	0.3388	0.6612	0.6276	0.8989	0.5185	0.9489	0.1091	-0.0500	0.0591	19
5	0.3388	0.6612	0.5537	0.7360	0.5185	0.9489	0.0352	-0.2129	-0.1777	41
6	0.3388	0.6612	0.6775	0.7859	0.5185	0.9489	0.1591	-0.1630	-0.0039	28
7	0.3388	0.6612	0.4796	0.8284	0.5185	0.9489	-0.0389	-0.1205	-0.1594	39
8	0.3388	0.6612	0.6486	1.0902	0.5185	0.9489	0.1301	0.1413	0.2714	1
9	0.3388	0.6612	0.5014	0.8177	0.5185	0.9489	-0.0171	-0.1313	-0.1483	38
…										
20	0.3388	0.6612	0.5235	0.9709	0.5185	0.9489	0.0050	0.0220	0.0270	23
21	0.3388	0.6612	0.5451	0.8532	0.5185	0.9489	0.0267	-0.0958	-0.0691	35
22	0.3388	0.6612	0.4300	0.8141	0.5185	0.9489	-0.0885	-0.1348	-0.2233	44
…										
30	0.3388	0.6612	0.5263	1.1132	0.5185	0.9489	0.0050	0.0220	0.0270	23
31	0.3388	0.6612	0.4311	1.1440	0.5185	0.9489	0.0267	-0.0958	-0.0691	35
32	0.3388	0.6612	0.5646	1.0688	0.5185	0.9489	-0.0885	-0.1348	-0.2233	44
…										
44	0.3388	0.6612	0.5494	0.7472	0.5185	0.9489	0.0310	-0.2017	-0.1707	40
45	0.3388	0.6612	0.5805	0.8876	0.5185	0.9489	0.0621	-0.0613	0.0008	27
46	0.3388	0.6612	0.5070	0.9046	0.5185	0.9489	-0.0114	-0.0443	-0.0558	33

C. Interpretation and Practical Implications

The integration of GPR–NSGA-II for Pareto front generation and Entropy-weighted MABAC for decision-making allows for a comprehensive and interpretable evaluation of competing machining strategies.

The selection of Trial 8 as the optimal solution represents a balanced trade-off, providing relatively high productivity with minimal electrode degradation—ideal for practical UV-EDM applications in precision tool manufacturing. The use of Entropy-derived weights also enhances the objectivity of the ranking process by reflecting the discriminative power of each criterion based on experimental variation.

This hybrid framework offers a replicable approach for multi-objective process optimization, particularly when subjective weighting is not feasible or when a balance between technical performance and operational costs must be achieved.

V. Conclusion

This study introduced a hybrid multi-objective optimization framework for UV-EDM, targeting the simultaneous maximization of MRR and minimization of EWR. A Box–Behnken Design (BBD) was employed to plan 46 experimental trials, and GPR models were developed to predict process responses with high fidelity.

The GPR models were integrated with the NSGA-II algorithm to generate a well-distributed Pareto front capturing the trade-offs between MRR and EWR. To facilitate the final selection, the MABAC method was applied to rank the Pareto-optimal solutions based on entropy-derived objective weights. Among the evaluated solutions, Trial 8 was identified as the

most balanced configuration, achieving a favorable compromise between machining productivity and electrode preservation.

The results demonstrate the effectiveness of combining GPR, NSGA-II, Entropy weighting, and MABAC for complex decision-making in advanced manufacturing. The proposed approach not only improves process performance but also offers a replicable and interpretable framework for multi-criteria optimization in other EDM and hybrid machining contexts.

ACKNOWLEDGMENT

This work was supported by Thai Nguyen University of Technology.

REFERENCES

[1] Z. Yin et al., "A novel EDM method using longitudinal-torsional ultrasonic vibration (LTV) electrodes to improve machining performance for micro-holes," Journal of Manufacturing Processes, vol. 102, pp. 231–243, 2023.

[2] W. Chenxue, T. Sasaki, and A. Hirao, "Observation of bubble behavior in EDM with ultrasonic vibration," Procedia CIRP, vol. 113, pp. 267–272, 2022.

[3] A. Hirao, H. Gotoh, and T. Tani, "Some effects on EDM characteristics by assisted ultrasonic vibration of the tool electrode," Procedia CIRP, vol. 68, pp. 76–80, 2018.

[4] Xu, J. Zhang, Y. Li, Q. Zhang, and S. Ren, "Material removal mechanisms of cemented carbides machined by ultrasonic vibration assisted EDM in gas medium," Journal of Materials Processing Technology, vol. 209, no. 4, pp. 1742–1746, 2009.

[5] J. Lei et al., "Ultrasonic vibration-assisted electrical discharge machining of enclosed microgrooves with laminated electrodes," Journal of Materials Research and Technology, vol. 30, pp. 9521–9530, 2024.

[6] J. Singh, R. Walia, P. Satsangi, and V. Singh, "FEM modeling of ultrasonic vibration assisted work-piece in EDM process," International Journal of Mechanic Systems Engineering, vol. 1, no. 1, pp. 8–16, 2011.

[7] D. Kremer, C. Lhiaubet, and A. Moisan, "A study of the effect of synchronizing ultrasonic vibrations with pulses in EDM," CIRP Annals, vol. 40, no. 1, pp. 211–214, 1991.

[8] G. S. Prihandana et al., "Effect of micro-powder suspension and ultrasonic vibration of dielectric fluid in micro-EDM processes—Taguchi approach," International Journal of Machine Tools and Manufacture, vol. 49, no. 12–13, pp. 1035–1041, 2009.

[9] Q. Xing, Z. Yao, and Q. Zhang, "Effects of processing parameters on processing performances of ultrasonic vibration-assisted micro-EDM," The International Journal of Advanced Manufacturing Technology, vol. 112, pp. 71–86, 2021.

[10] Y. Wang et al., "Analysis of material removal and surface generation mechanism of ultrasonic vibration–assisted EDM," The International Journal of Advanced Manufacturing Technology, vol. 110, pp. 177–189, 2020.

[11] C. Praneetpongrung et al., "Effects of the EDM combined ultrasonic vibration on the machining properties of Si3N4," Materials Transactions, vol. 51, no. 11, pp. 2113–2120, 2010.

[12] Y. Wang, L. Fan, J. Shi, Y. Dong, and Z. Fu, "Effect of cavitation on surface formation mechanism of ultrasonic vibration-assisted EDM," The International Journal of Advanced Manufacturing Technology, vol. 124, no. 10, pp. 3645–3656, 2023.

[13] Y.-C. Lin, F.-P. Chuang, A.-C. Wang, and H.-M. Chow, "Machining characteristics of hybrid EDM with ultrasonic vibration and assisted magnetic force," International Journal of Precision Engineering and Manufacturing, vol. 15, pp. 1143–1149, 2014.

[14] M. T. Shervani-Tabar, K. Maghsoudi, and M. R. Shabgard, "Effects of simultaneous ultrasonic vibration of the tool and the workpiece in ultrasonic assisted EDM," International Journal for Computational Methods in Engineering Science and Mechanics, vol. 14, no. 1, pp. 1–9, 2013.

[15] Y. Zhang and B. Xie, "Investigation on hole diameter non-uniformity of hole arrays by ultrasonic vibration-assisted EDM," The International Journal of Advanced Manufacturing Technology, vol. 112, pp. 3083–3091, 2021.

[16] M. T. Shervani-Tabar, A. Abdullah, and M. R. Shabgard, "Numerical and experimental study on the effect of vibration of the tool in ultrasonic assisted EDM," The International Journal of Advanced Manufacturing Technology, vol. 32, pp. 719–731, 2007.

[17] M. Iwai, S. Ninomiya, and K. Suzuki, "Improvement of EDM properties of PCD with electrode vibrated by ultrasonic transducer," Procedia CIRP, vol. 6, pp. 146–150, 2013.

[18] M. M. Sundaram, G. B. Pavalarajan, and K. P. Rajurkar, "A study on process parameters of ultrasonic assisted micro EDM based on Taguchi method," Journal of Materials Engineering and Performance, vol. 17, pp. 210–215, 2008.

[19] M. Shabgard et al., "Ultrasonic assisted EDM: Effect of the workpiece vibration in the machining characteristics of FW4 Welded Metal," Frontiers of Mechanical Engineering, vol. 6, pp. 419–428, 2011.

[20] Y. Dong, J. Liu, G. Li, and Y. Wang, "Thermodynamic simulation modeling analysis and experimental research of vertical ultrasonic vibration assisted EDM," The International Journal of Advanced Manufacturing Technology, vol. 119, no. 7, pp. 5303–5314, 2022.

[21] J. Xu et al., "Multi-objective parameter optimization of ultrasonic vibration–assisted micro-EDM of Ti-6Al-4V alloys," Journal of Vibration and Control, vol. 30, no. 7–8, pp. 1818–1828, 2024.

[22] A. Abdullah and M. R. Shabgard, "Effect of ultrasonic vibration of tool on electrical discharge machining of cemented tungsten carbide (WC-Co)," The International Journal of Advanced Manufacturing Technology, vol. 38, pp. 1137–1147, 2008.

[23] A. Gholipoor, M. R. Shabgard, M. Mohammadpourfard, and H. Abbasi, "Comparative study of ultrasonic vibrations assisted EDM and magnetic field assisted EDM processes," Iranian Journal of Mechanical Engineering Transactions of the ISME, vol. 21, no. 1, pp. 45–64, 2020.
[24] Alinezhad, A., New methods and applications in multiple attribute decision making (MADM). 2019: Springer.
[25] Hieu, T.T., N.X. Thao, and L. Thuy, Application of MOORA and COPRAS Models to Select Materials for Mushroom Cultivation. Vietnam Journal of Agricultural Sciences, 2019. 17(4): p. 32-2331.

Contribution of Individual Authors to the Creation of a Scientific Article (Ghostwriting Policy)

The authors equally contributed in the present research, at all stages from the formulation of the problem to the final findings and solution.

Sources of Funding for Research Presented in a Scientific Article or Scientific Article Itself

No funding was received for conducting this study.

Conflict of Interest

The authors have no conflicts of interest to declare that are relevant to the content of this article.